2nd International Symposium on Magnetic Beaing
July 12-14, 1990, Tokyo, Japan

A SELF-EXCITED VIBRATION OF MAGNETIC BEARING SYSTEM WITH FLEXIBLE STRUCTURE

I.SATOH*1, C.MURAKAMI*2, A.NAKAJIMA*3 and Y.KANEMITSU*1

*1 Ebara Research Co.Ltd, Honfujisawa, Fujisawa 251, Japan
*2 Tokyo Metropolitan Institute of Technology, Hino, Tokyo 191, Japan
*3 National Aerospace Laboratory, Chofu, Tokyo 182, Japan

Abstract

A self-excited vibration with two different frequencies was observed on our 4-axis-active type magnetic bearing system which has been developed for high speed rotating machinery. In this paper, we discuss the cause and mechanism of the self-excited vibration. Experiments indicated that the cause of the self-excited vibration is interaction between nonlinearity of the electromagnet system and flexibility of the structure. Clarification on the mechanism of this self-excited vibration was made through analysis with nonlinear model, applying a method wherein both the root-locus method and a describing function method were used.

1. Introduction

It is well known that self-excited vibration in passive axis of magnetic bearing may be caused by increasing of internal damping when the rotor is driven over critical speed. Shimizu[1] and Kawamoto[2] investigated the cause of the self-excited vibration, and they obtained the same results indicating that the self-excited vibration is caused by energy loss such as eddy current loss act as internal damping. On the other hand, another type self-excited vibration may occurs even in the active-axis of magnetic bearing, if the magnetic bearing system has flexible structures. Since cause of the self-excited vibration is not clarified, it is difficult to obtaining stable high speed rotation in magnetic bearing system with flexible structures. A self-excited vibration with two different frequencies was observed on our 4-axis-active type magnetic bearing system which has been developed for high speed rotating machinery.

In this paper, we discuss the cause and mechanism of the self-excited vibration. The experimental results and computer simulations proved that the self-excited vibration is caused by interaction between nonlinearity of electromagnet systems and structural flexibility. The self-excited vibration mechanism is clarified by applying the root-locus method and approximate dual-input describing function method.

2. Characteristics of the self-excited vibration

To summarize the main characteristics of the self-excited vibration obtained from experiments, we have following:

(1) The self-excited vibration is caused by relatively low-level disturbance, if loop gains are set at relatively high value.

(2) Even if the loop gains are set at relatively low-level, high-level disturbance such as hammering causes the self-excited vibration.

Figure 1 shows an example of the self-excited vibration observed in case of non-rotation. In this wave form, high frequency vibration may be first bending mode of the stator shaft, and low frequency vibration may be rigid mode of the rotor. Thus, the self-excited vibration is composed of two vibrations with different frequencies and become continuous vibration (limit cycle) in case of non-rotation state.

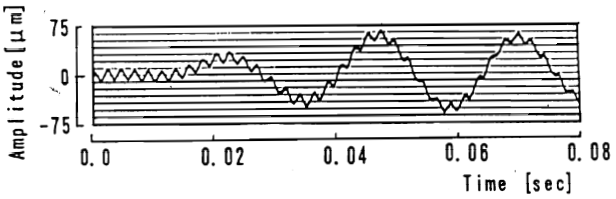

Fig.1 An example of the self-excited vibration

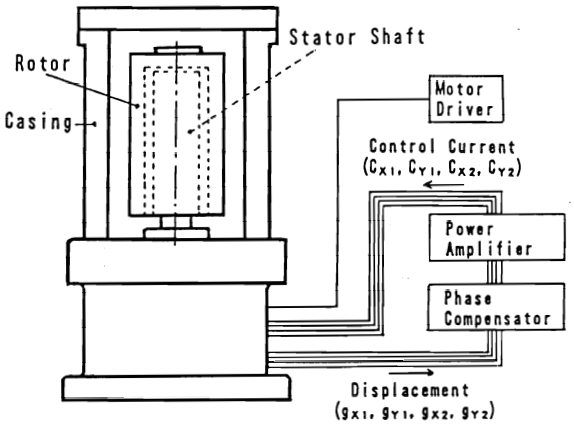

Fig.2 Four-axis-active type magnetic bearing system

3. Magnetic bearing system

A magnetic bearing system, shown in Fig.2, is consist of 4-axis-active type magnetic bearing which is located inside of a casing, its compensators and its power amplifiers which generate control currents. In the following, we give brief explanations and models of them for analysis.

3.1 Four-axis-active type magnetic bearing

3.1.1 Mechanical structure The mechanical structure of the 4-axis-active type magnetic bearing is shown in Fig.3, where the rotor has hanging bell shape and stator is a cantilever. The 4-axis-active type magnetic bearing is consist of two radially-active type magnetic bearings which are located on both side of the high speed motor. The radially-active type magnetic bearings contain permanent magnets and electromagnets. The rotor is passively stabilized in the axial direction by the restoring attractive force of the permanent magnets. However, the magnetic bearing even has imbalance stiffness, which is expressed as a negative spring constant, in the radial direction due to the attractive force of the permanent magnets. The electromagnets regulate radial clearance between rotor and stator and cancel the radial imbalance stiffness. Static characteristics for the rotor are shown in Table 1.

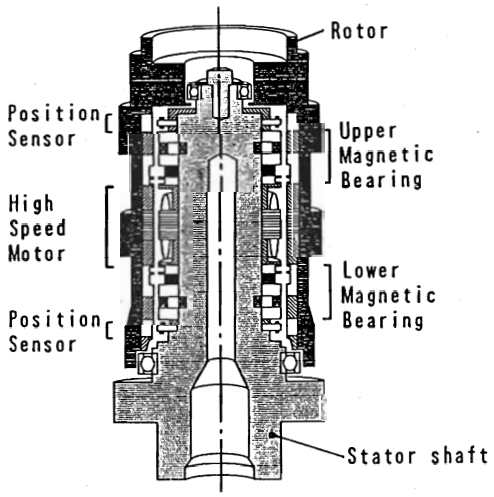

Fig.3 Mechanical structure of the 4-axis-active type magnetic bearing

3.1.2 Model of the dynamics Since the 4-axis-active type magnetic bearing is outer-rotor type, the first-bending-mode frequency of the rotor could be set at a rather high value, and only the rigid mode should be considered for the rotor. However, a first-bending-mode frequency of the stator shaft, which swings largely at the top part of the shaft but little at the bottom, is in the rotational region. Therefore, we adopt the simplified 2-DOF model shown in Fig.4, where only the radial motion of the upper side magnetic bearing is considered. Modal coefficients of the stator shaft are shown in Table 2.

Table 1 Static characteristics

Rotor Mass	$M = 5.7$	[kg]
Rotor Inertia		
Spin Axis	$I_p = 15.9\times10^{-3}$	[kg・m²]
Radial Axis	$I_d = 31.5\times10^{-3}$	[kg・m²]
Ratio	$\gamma = I_p/I_d = 0.504$	
Radial Unbalance Stiffness	$K_u = 12.7\times10^{5}$	[N/m]
Axial Stiffness	$K_z = 2.46\times10^{5}$	[N/m]

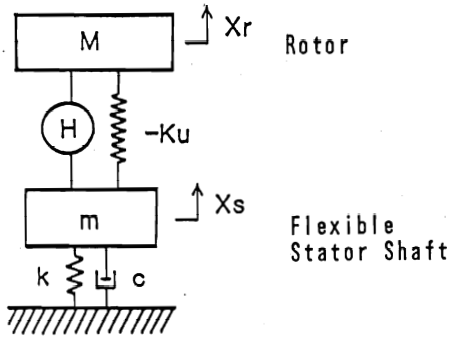

H : Controller

−Ku : Unbalance Stiffness

Fig.4 Dynamical model

Table 2 Modal coefficients of the stator shaft

Mass	$m = 2.2$	[kg]
Damping Coefficient	$c = 209$	[Ns/m]
Stiffness	$k = 2.21\times10^{7}$	[N/m]
Resonace Frequency	$\omega_n = 504$	[Hz]
Damping ratio	$\zeta = 0.015$	

3.2 Compensators

The independent control method for each axis, which does not separate the motion into translational and rotational modes, was adopted for simplicity of the control system. Every axis has a same phase compensator, whose transfer function is as follows.

$$H(s)=\frac{1+T_1 s}{1+T_2 s} \qquad (T_1>T_2)$$

3.3 Electromagnet system

An electromagnet system for the magnetic bearing, which is composed of a power amplifier

and electromagnetic coils, has a wide range bandwidth generally. Therefore, transfer functions for the electromagnet system have as far been expressed by constant element or first-order lag element at most. These models are valid when the low frequency vibration problems such as rigid mode are discussed. However, characteristics of the electromagnet system tend to become worse in high frequency region. Therefore, nonlinear model for electromagnet system should be adopted when the system includes flexible mode of which resonance frequency is several hundreds Hz.

3.3.1 Experimental results Figure 5 shows a circuit diagram of the power amplifier used in this system. The power amplifier is push-pull type and utilize 24 [V] power supply. Figure 6 shows frequency characteristic curves of the electromagnet system, when the input voltage was changed in three steps. It is obvious from this figure that the electromagnet system has nonlinearity in which phase characteristic becomes worse in the case where high-frequency, large amplitude signals are applied.

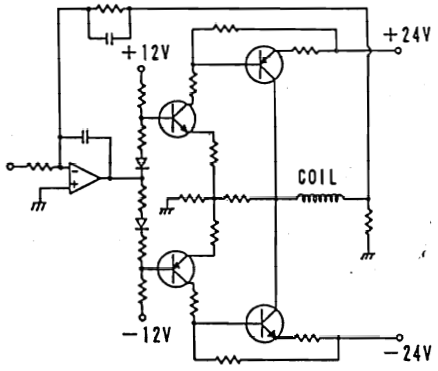

Fig.5 Circuit diagram of the power amplifier

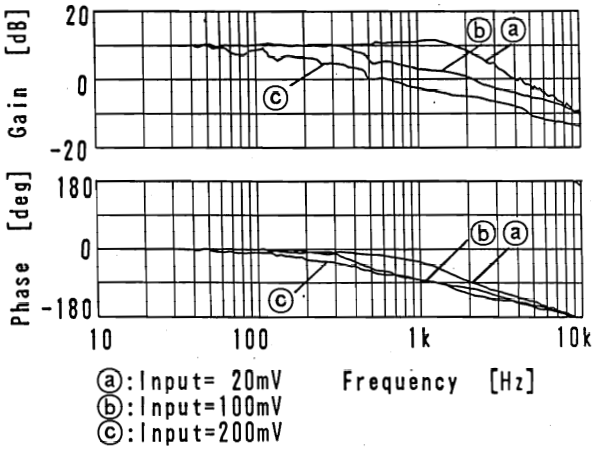

Fig.6 Frequency characteristic curves of the electromagnet system (Experiments)

3.3.2 Model for electromagnet system Considering the experimental results of electromagnet system, we adopted the model shown in Fig.7. The model consist of a saturation element and 2nd-order lag element, which are negatively fedback by constant gain element K_F.[3] Figure 8 shows frequency characteristic curves for the electromagnet system obtained form calculation by using the model. This figure proves validity of the model.

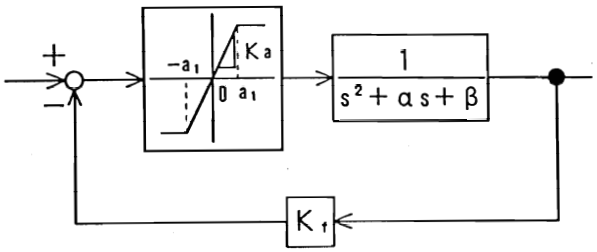

Fig.7 Nonlinear model of the electromagnet system

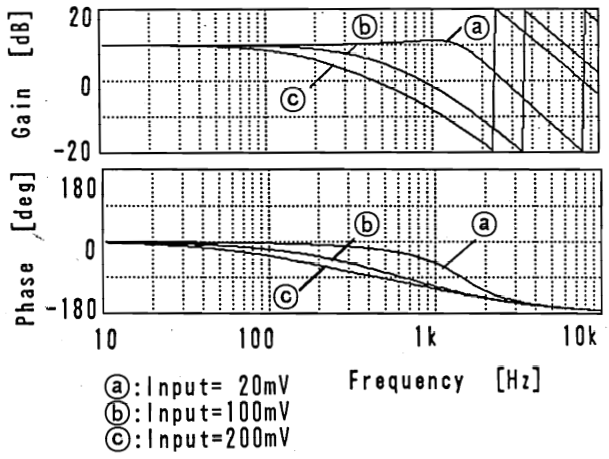

Fig.8 Frequency characteristic curves of the electromagnet system (Simulations)

4. Simulations

Figure 9 shows a block diagram of the whole system including nonlinear electromagnet system and a flexible structure. Figure 10(a) shows the wave forms of the self-excited vibration obtained from experiments. In this figure, upper side wave form represents relative displacement between rotor and stator shaft, and lower side wave form represents control current. As it is clear from this figure, both signals do continuous vibration which are composed of two different frequency vibrations. Figure 10(b) shows simulation results used the system shown in Fig.9. Similarly to the experimental results, both signals of the simulation show continuous vibration including two different frequency vibrations.

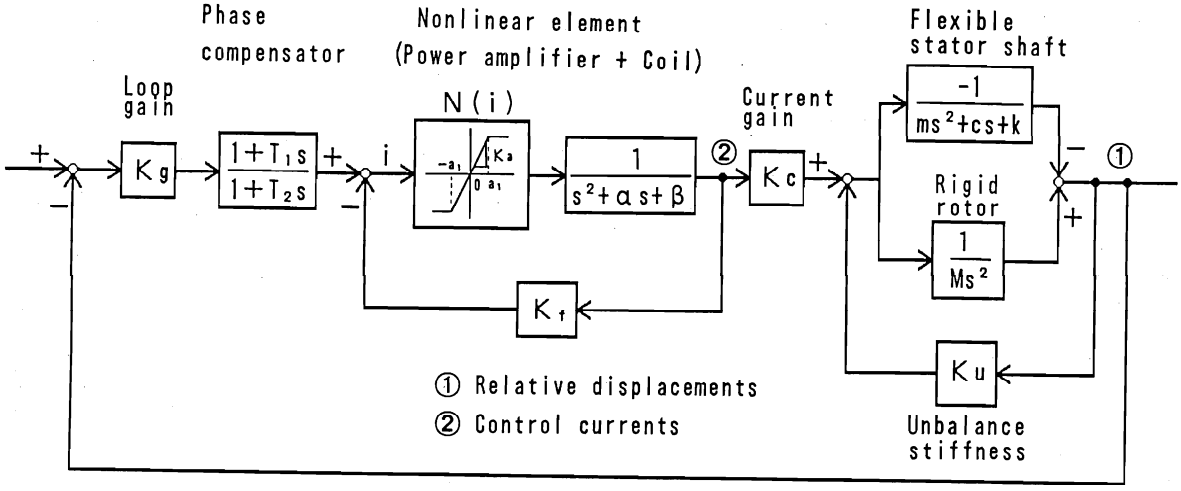

Fig.9 Block diagram of the system

Because of modeling approximation, the amplitude of the high frequency vibration in simulation is about one third times as small as the experimental results, though the amplitude of the low frequency vibration indicates good agreement between simulations and experiments.

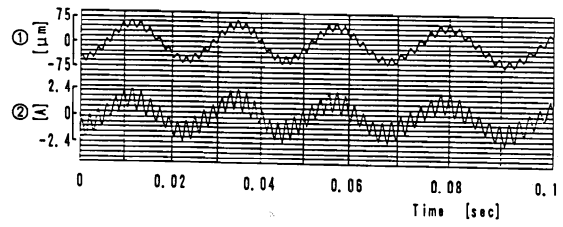

(a) Experimental results

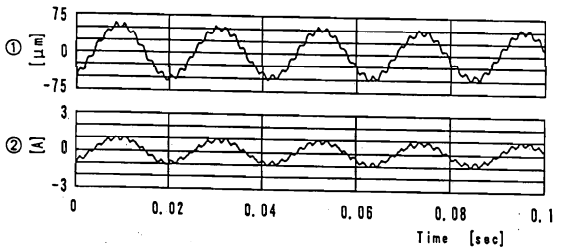

(b) Simulations

① Relative displacements
② Control currents

Fig.10 The self-excited vibration

5. Analysis for self-excited vibration

By using root-locus method and describing function(DF) method, occurrence mechanism of the self-excited vibration will be discussed.

5.1 Root-loci in nonlinear domain

The DF of the saturation element is represents only by change of gain, which depends on the amplitude of input signal. Therefore, root-loci of the system in nonlinear domain can be calculated by replacing the saturation element by linear gain element N. Figure 11 shows the root-loci of a rigid mode and flexible mode. In this figure, the root-loci by varying the loop gain Kg are shown by dotted lines and marks show the operating point in the linear domain. Solid lines show the change of characteristic roots by varying the ψ($=N/K_a$) at the operating points. The relationship between ψ and the stability of the two modes are clarified from this figure as follows.

(1) Stable region of the rigid mode

$$0.066 < \psi < 1 \qquad (1)$$

(2) Stable region of the flexible mode

$$\psi < 0.092 \ , \ 0.224 < \psi < 1 \qquad (2).$$

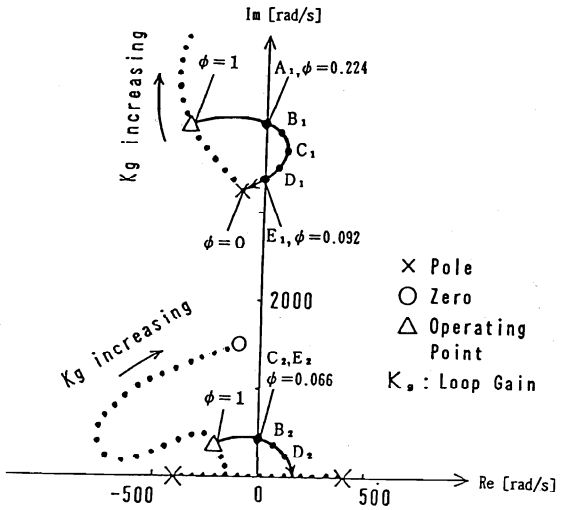

Fig.11 Root-loci of the system

5.2 Approximate dual-input describing function (ADIDF) method

In order to obtain the relationship between amplitude of the input signal and stability of the system, the value ψ of saturation element will be calculated by utilizing DF method. As is mentioned earlier, this self-excited vibration is composed of two different frequency oscillations so that dual-input describing function(DIDF), should be calculated. The DIDF method is based on consideration of two sinusoids as a input, shown in Eq.(3), being applied to the nonlinear element.

$$i = a_0 \sin(\omega t) + b_0 \sin(\beta t) \qquad (3)$$

Since the frequency of the two vibrations separate enough(ω =530Hz, β =40Hz), an ADIDF method could be utilized in this case. Assume that change of the low frequency component can be neglected while one any cycle of the high frequency component, the input signal is considered as shown in Eq.(4), which is composed of DC-bias and high-frequency oscillatory component.

$$i = a_0 \sin(\omega t) + B_D \qquad (4)$$

Then, output signal from the nonlinear element can be approximated as

$$y = \frac{A_0}{2} + a_1 \sin(\omega t) \qquad (5)$$

By adopting Fourier analysis to these equations, next two equivalent gains can be defined.

(1) Equivalent gain for DC component of the input signal (Equivalent DC gain)

$$K_{ed} = A_0 / 2B_D \qquad (6)$$

(2) Equivalent gain for sinusoidal component of the input signal

$$K_{ea} = a_1 / a_0 \qquad (7)$$

These two equivalent gains are not independent each other but dependent on each amplitude of the high and low frequency component including of signal. These gains for saturation element are obtained as follows.

$$K_{ed} = \frac{K_a}{\pi}\left[\phi_1 + \phi_2 + \frac{a_0}{B_D}(\cos\phi_2 - \cos\phi_1) + \frac{a_1}{B_D}(\phi_2 - \phi_1)\right] \qquad (8)$$

$$K_{ea} = \frac{2K_a}{\pi}\left[\frac{a_1 - B_D}{a_0}\cos\phi_1 + \frac{a_1 + B_D}{a_0}\cos\phi_2 + \frac{1}{4}\{2(\phi_1 + \phi_2) - (\sin 2\phi_1 + \sin 2\phi_2)\}\right] \qquad (9)$$

where $\phi_1 = \sin^{-1}\left(\frac{a_1 - B_D}{a_0}\right)$, $\phi_2 = \sin^{-1}\left(\frac{a_1 + B_D}{a_0}\right)$

5.2.1 ADIDF for low frequency component

Boyer [4] developed ADIDF for low frequency component of input signal by applying above-mentioned equivalent DC gain K_{ed}. Average value of output signal from nonlinear element can be calculated by product of B_D and K_{ed}. The "representative output wave" is determined to join the obtained value by smooth line as shown in Fig.12. By adopting the Fourier analysis to this wave form directory, the amplitude of fundamental wave(b_1) is obtained. Therefore, ADIDF for high frequency component is calculated by next equation.

$$N_r = b_1 / b_0 \qquad (10)$$

Figure 13 shows the ADIDF for saturation element calculated by Boyer's method. If each amplitude ratio ε_r (= b_0/a_1), ε_f (= a_0/a_1) of low and high frequency component in input signal are known, ADIDF ratio of low frequency component ψ_r (=N_r/K_a) can be obtained from this figure. The shadowed portion in this figure is defined as a stable region of the low frequency component by Eq.(1) obtained form root-loci shown in Fig.11.

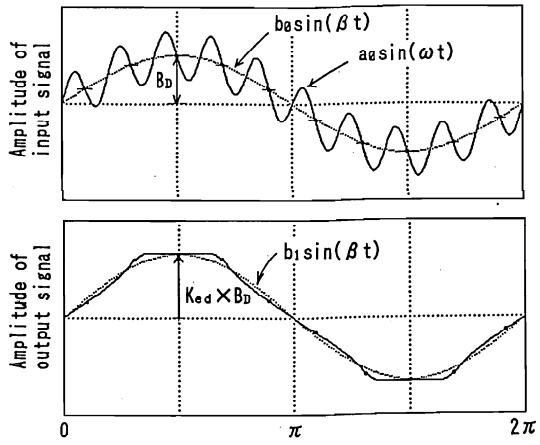

Fig.12 Representative output wave for low frequency component

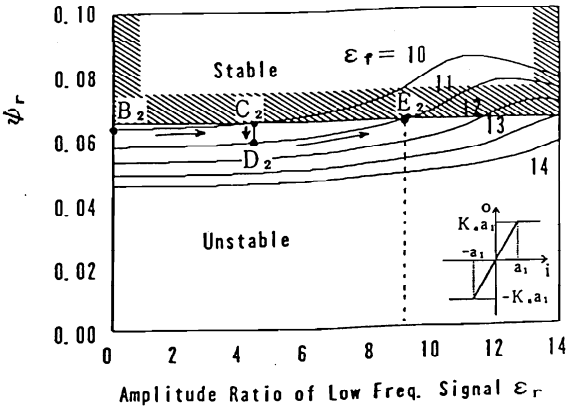

Fig.13 ADIDF of saturation element for low frequency component

5.2.2 ADIDF for high frequency component The equivalent gain for high frequency component K_{ea} can be calculated from Eq.(7), if the DC value B_D is fixed. Then, we regard the low frequency component as a DC-bias, because the change of low frequency component in a cycle of the high frequency component is so slow that we can neglect it. Since K_{ea} is changed with B_D, the change of K_{ea} in a cycle of low frequency is shown in Fig.14, where K_{ea} indicates maximum value when the amplitude of the low frequency component is zero and indicates minimum value when the amplitude of the low frequency component is maximum. In this analysis, we defined the average of K_{ea} as an ADIDF of the high frequency component. Figure 15 shows the ADIDF ration for high frequency component ψ_f ($=N_f/K_a$) obtained from above-mentioned method. The shadowed portion in this figure shows stable region of the ADIDF for high frequency component determined by Eq.(2).

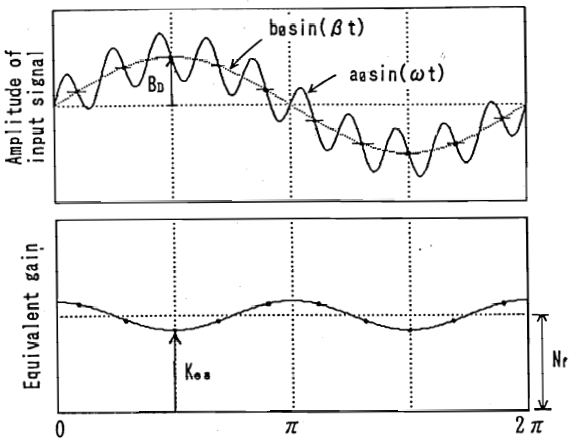

Fig.14 Equivalent gain for high frequency component

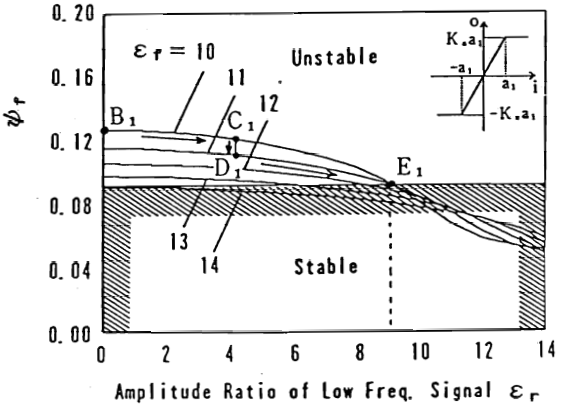

Fig.15 ADIDF of saturation element for high frequency component

5.3 Occurrence mechanism of the self-excited vibration

By using Figs.11,13 and 15, the process from resonance vibration of stator shaft to the self-excited vibration is explained as follows;

(1) If the stator shaft is excited by some disturbance as impulse force, the ADIDF for flexible mode (corresponding to the high frequency component) ψ_f is defined according to the amplitude of the vibration. As it is obvious from Fig.11, the characteristic roots of flexible mode exist in left-half plane within the range of $1 > \psi_f > 0.224$ so that the vibration is damped. However, if the amplitude of the vibration becomes larger, the ψ_f decrease under 0.224. Therefore, the characteristic roots of flexible mode moves into right-half plane and the vibration tends to diverge.

(2)Now we consider the condition that $\varepsilon_f = 10$, $\varepsilon_r = 0$, then ψ_f and ψ_r are pointed by B_1, B_2 in Figs.12 and 14, respectively. As it is clear from these figures, both the flexible mode and the rigid mode(corresponding to the low frequency component) is unstable. Therefore, both vibrations tend to diverge.

(3)Firstly, we pay attention to the rigid mode. As it is clear from Fig.13, ψ_r increases with increment of ε_r in the region of $0 < \varepsilon_r < 10$ when ε_f is constant. In case of $\varepsilon_f = 10$, ψ_r reaches the threshold between stable and unstable region when ε_r is about 4.5(point C_2). This point is a kind of equilibrium point, because if ε_r increases more than 4.5, the characteristic roots of rigid mode moves into stable region therefore the amplitude of the rigid mode tends to damp. On the other hand, if ε_r decrease less than 4.5 due to decrease of amplitude of the rigid mode, the characteristic roots of the rigid mode come back to the unstable region therefore the amplitude of the rigid mode tends to diverge. Consequently, the amplitude of the rigid mode keep balance in this point.

(4)Secondly, as it is clear from Fig.15, the flexible mode is still unstable in point C_1 (corresponding to the point C_2 in Fig.13) so that the amplitude of the flexible mode tends to increase. Now we assume that the amplitude of flexible mode increase up to $\varepsilon_f = 10$(point D_1). As seen from Fig.13, the rigid mode becomes unstable again at point D_2(corresponding to the point D_1 in Fig.15), because ψ_r decreases with increment of ε_f when ε_r is constant.

(5)Thus, amplitude of the both rigid and flexible mode increase as they are influenced each other. Consequently, they balance at the boundary point (E_1, E_2) between stable and unstable region, when $\psi_r = 9$ and $\psi_f = 11$. As it is clear from Fig.11 that both E_1 and E_2 are located on the imaginary axis, continuous vibration including two frequency components occurs.

Considering the circumstances mentioned above, it is obvious that rigid mode is caused by flexible mode. And the flexible mode becomes stable limit cycle, when ψ_f decreases less than 0.224 due to the increasing of amplitude of the vibration, in case that the disturbance causing the vibration is not continuous, but impactive. Therefore, the self-excited vibration with two different frequency will be occurred. However, the rigid mode tends to toward unstable region when the amplitude of the flexible mode becomes large, though the flexible mode tends to toward stable region when the amplitude of the rigid mode becomes large. Therefore, if the amplitude of flexible mode becomes larger than ψ_f =0.092 due to forced disturbance such as unbalanced force, rigid mode becomes unstable.

6. Conclusions

In this paper, we discuss the cause and mechanism of the self-excited vibration occurs on our 4-axis-active type magnetic bearing which has been developed for high speed rotating machinery. The results of this research are summarized as follows.

(1)The self-excited vibration caused by interaction between flexibility of the stator shaft and nonlinearity of the electromagnet system in which phase characteristic becomes worse in the case where high-frequency, large-amplitude signals are applied.

(2)The self-excited vibration contain two different frequency vibrations, and the rigid mode(low frequency component) is caused by flexible mode (high frequency component).

(3)The rigid mode vibration has apprehension to become unstable in case that the flexible mode vibration become large, though the flexible mode surely becomes stable limit cycle regardless of the amplitude of rigid mode vibration.

7. Acknowledgment

The authors would like to express special thanks to Mr.Makoto IMAI, then a graduate student of Tokyo Denki University, for assistance in the simulations and experiments.

8. References

[1] H.Shimizu, H.Ozawa, O.Taniguchi, Trans. Jpn. Soc. Mech. Eng.,(in Japanese), Vol.36, No.290, 1(1970), p.1656.

[2] H.Kawamoto, K.Kikuchi, Trans. Jpn. Soc. Mech. Eng., (in Japanese), Vol.47, No.419, C(1981), p.849.

[3] A.Nakajima, M.Imai, I.Satoh, J.Nagahiro and C.Murakami, Proc. China-Japan Symp. on Mechatronics, (1988), p.63

[4] J.Gibson, "Nonlinear Automatic Control", McGraw-Hill Book Company, New York, 1963.